

Inhibition Effect of 3-bromo-2-phenylimidazol[1,2- α]pyridine towards C38 Steel Corrosion in 0.5M H₂SO₄ Solution.

R. Salghi^{1,*}, A. Anejjar¹, O. Benali², S. S. Al-Deyab³, A. Zarrouk⁴, M. Errami¹, B. Hammouti^{3,4,*}, N Benchat⁴

¹ Laboratory of Environmental Engineering and Biotechnology, ENSA, Université Ibn Zohr, PO Box 1136, 80000 Agadir, Morocco

² Département de Biologie, Faculté des sciences, Université Dr. Tahar Moulay – Saïda- Algérie

³ Petrochemical Research Chair, Chemistry Department, College of Science, King Saud University, P.O. Box 2455, Riyadh 11451, Saudi Arabia

⁴ LCAE-URAC 18, Faculty of Science, University of Mohammed Premier, Po Box 717 60000 Oujda, Morocco

*E-mail: r.salghi@uiz.ac.ma & hammoutib@gmail.com

Received: 13 January 2014 / Accepted: 27 January 2014 / Published: 23 March 2014

The inhibition effect of 3-bromo-2-phenylimidazol[1,2- α]pyridine on the corrosion behaviour of C38 steel in 0.5M H₂SO₄ solution was investigated using weight loss, potentiostatic polarization and electrochemical impedance spectroscopy methods. The inhibition efficiency increased as the concentration of the inhibitors was increased. The effect of temperature on corrosion inhibition was investigated by electrochemical impedance spectroscopy method and thermodynamic parameters were calculated. Potentiodynamic polarization measurements show that the studied inhibitor acts as mixed inhibitor. The adsorption of inhibitors on C38 steel surface obeys Langmuir adsorption isotherm.

Keywords: C38steel; 3-bromo-2-phenylimidazol[1,2- α]pyridine, acid solution; inhibition corrosion; adsorption.

1. INTRODUCTION

The study of corrosion of steel and iron in acid media remains a global scientific problem which affects all kinds of industries. The economic cost of corrosion is enormous and has been estimated to be in the range of 2–4 % of an industrialized country's gross national product. In the field of combating corrosion, both economic and scientific considerations are involved. Acids are widely used in industrial processes such as pickling, cleaning, decaling, and oil well acidizing. Because of the aggressivity of acid, solutions inhibitors are used to reduce the rate of dissolution of metals [1-2]. In

general, an inhibitor retards corrosion reactions by: adsorption of ions/molecules on metal surface, altering the anodic and/or cathodic reaction, and decreasing the diffusion rate of reactants to the metal surface [3]. Corrosion inhibition is reversible and a minimum concentration of the inhibiting compound is required to maintain the inhibiting surface film. The effectiveness of inhibitor depends on solution corrosivity, concentration, and temperature. It is well known that the organic inhibitors having heteroatom –O, N, S are the best corrosion inhibitors in acid solution as they have higher basicity [4–9]. These heteroatoms act as active centre for adsorption on metal surface [10].

In this work, 3-bromo-2-phenylimidazol[1,2- α]pyridine named BPP (fig.1) was evaluated as chemical corrosion inhibitor for acidic environment. Weight loss tests and electrochemical measurements were applied to test the inhibitory properties of this compound in C38 steel immersed in 0.5 M H₂SO₄.

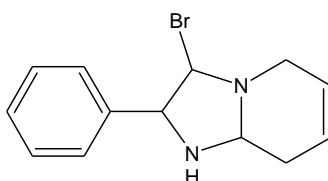


Figure 1. Molecular structure of 3-bromo-2-phenylimidazol[1,2- α]pyridine

2. MATERIALS AND METHODS

2.1. Electrochemical tests

The electrochemical study was carried out using a potentiostat PGZ100 piloted by Voltmaster software. This potentiostat is connected to a cell with three electrode thermostats with double wall (Tacussel Standard CEC/TH). A saturated calomel electrode (SCE) and platinum electrode were used as reference and auxiliary electrodes, respectively. The material used for constructing the working electrode was the same used for gravimetric measurements. The surface area exposed to the electrolyte is 0.04 cm².

Potentiodynamic polarization curves were plotted at a polarization scan rate of 0.5 mV/s. Before all experiments, the potential was stabilized at free potential during 30 min. The polarisation curves are obtained from –800 mV to –200 mV at 298 K. The solution test is there after de-aerated by bubbling nitrogen. Gas bubbling is maintained prior and through the experiments. In order to investigate the effects of temperature and immersion time on the inhibitor performance, some test were carried out in a temperature range 298–328 K.

The electrochemical impedance spectroscopy (EIS) measurements are carried out with the electrochemical system (Tacussel), which included a digital potentiostat model Voltalab PGZ100 computer at E_{corr} after immersion in solution without bubbling. After the determination of steady-state current at a corrosion potential, sine wave voltage (10 mV) peak to peak, at frequencies between 100 kHz and 10 mHz are superimposed on the rest potential. Computer programs automatically controlled

the measurements performed at rest potentials after 0.5 hour of exposure at 298 K. The impedance diagrams are given in the Nyquist representation. Experiments are repeated three times to ensure the reproducibility.

2.2. Weight loss measurements

Coupons were cut into $2 \times 2 \times 0.08 \text{ cm}^3$ dimensions having composition (0.179% C, 0.165% Si, 0.439% Mn, 0.203% Cu, 0.034% S and Fe balance) are used for weight loss measurements. Prior to all measurements, the exposed area was mechanically abraded with 180, 320, 800, 1200 grades of emery papers.

The specimens are washed thoroughly with bidistilled water, degreased and dried with ethanol. Gravimetric measurements are carried out in a double walled glass cell equipped with a thermostated cooling condenser. The solution volume is 80 cm^3 . The immersion time for the weight loss is 6 h at 298K.

3. RESULTS AND DISCUSSION

3.1. Potentiodynamic polarization curves

Potentiodynamic polarization data of various concentrations of BPP are shown as the Tafel plots for C38 steel in 0.5 M H_2SO_4 in Figure 2.

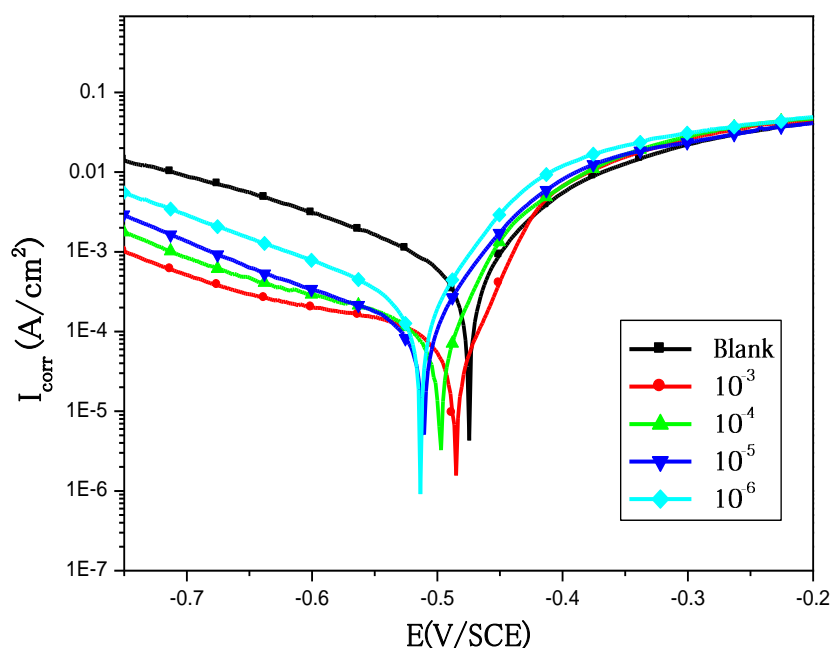


Figure 2. Potentiodynamic polarization curves of C38 steel in 0.5M H_2SO_4 in the presence of different concentrations of BPP

The corrosion kinetic parameters such as corrosion potential (E_{corr}), corrosion current density (I_{corr}), cathodic Tafel slopes (b_c) were derived from these curves and are given in Table 1. The values of inhibition efficiency ($IE_{I_{\text{corr}}}$ %) were calculated using the following equation:

$$IE_{I_{\text{corr}}} (\%) = \frac{(I_{\text{corr}}^0 - I_{\text{corr}})}{I_{\text{corr}}^0} \times 100 \quad (1)$$

where I_{corr}^0 and I_{corr} are the values of corrosion current densities of C38 steel without and with the additive, respectively, which were determined by extrapolation of the cathodic Tafel lines to the corrosion potential E_{corr} .

The data in Table 1 indicate that in both cases I_{corr} values gradually decreased with the increase of the inhibitor concentration with respect to the blank. The values of the cathodic Tafel slopes, b_c , were found to vary slightly with the exception of the lowest concentration. Thus, the presence of the inhibitor does not affect the cathodic slopes (b_c). This indicates that addition of BPP does not modify the mechanism of the proton discharge reaction. The values of inhibition efficiency (IE %) increase with inhibitor concentration reaching a maximum value (86.83 %) at 10^{-3} M.

Table 1. Electrochemical parameters of C38 steel at various concentrations of BPP in 0.5M H_2SO_4 and corresponding inhibition efficiency.

Inhibitor	Conc. (M)	$-E_{\text{corr}}$ (mV/SCE)	I_{corr} ($\mu\text{A cm}^{-2}$)	$-b_c$ (mV dec $^{-1}$)	$IE_{I_{\text{corr}}}$ (%)
Blank	1.0	478	1860	189	----
BPP	1×10^{-3}	487	245	226	86.83
	1×10^{-4}	497	360	203	80.64
	1×10^{-5}	511	480	171	74.19
	1×10^{-6}	513	570	137	69.35

3.2. Electrochemical impedance spectroscopy measurements

Nyquist plots of C38 steel in 0.5 M H_2SO_4 in the presence and absence of additive are given in Figure 3. These curves have obtained after 0.5 h of immersion in the corresponding solution.

All the plots display a single capacitive loop. Impedance parameters derived from the Nyquist plots, percent inhibition efficiencies, IE_{R_t} (%) and the equivalent circuit diagram are given in Table 3 and Figure 4, respectively.

The values of R_t were given by subtracting the high frequency impedance from the low frequency one as follow [11]:

$$R_t = Z_{re}(\text{at low frequency}) - Z_{re}(\text{at high frequency}) \quad (2)$$

The values of electrochemical double layer capacitance C_{dl} were calculated at the frequency f_{max} , at which the imaginary component of the impedance is maximal ($-Z_{\text{max}}$) by the following equation [12]:

$$C_{dl} = \frac{1}{2\pi f_{\text{max}} R_t} \quad (3)$$

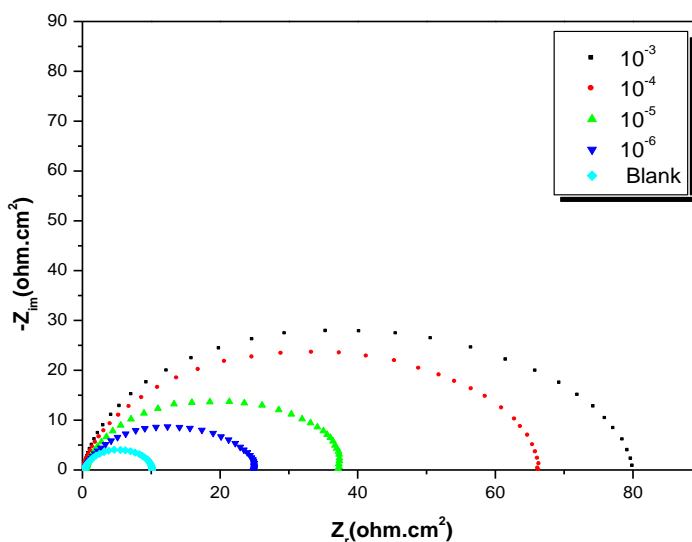


Figure 3. Nyquist diagrams for C38 steel electrode with and without BPP at E_{corr} after 30 min of immersion.

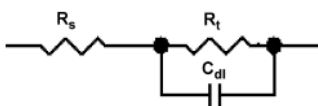


Figure 4. The electrochemical equivalent circuit used to fit the impedance spectra.

The percent inhibition efficiency is calculated by charge transfer resistance obtained from Nyquist plots, according to the equation :

$$EI_{R_t} (\%) = \frac{R_t - R_t^0}{R_t} \times 100 \tag{4}$$

where R_t and R_t^0 are the charge transfer resistance values without and with inhibitor, respectively.

Table 2. Electrochemical Impedance parameters for corrosion of C38 steel in acid medium at various contents of BPP

Inhibitor	Conc. (mol/l)	R_t ($\Omega.cm^2$)	f_{max} (Hz)	C_{dl} ($\mu F/cm^2$)	EI_{R_t} (%)
Blank	1.0	10	158	1×10^{-4}	----
BPP	1×10^{-3}	80	63	3.16×10^{-5}	87.50
	1×10^{-4}	66	79	3.05×10^{-5}	84.85
	1×10^{-5}	37	10	4.3×10^{-4}	72.97
	1×10^{-6}	25	63	1.01×10^{-4}	60.00

As can be seen from this table the increase in resistance in the presence of BPP, compared to H_2SO_4 , alone is related to the corrosion protection effect of the molecules. The value of C_{dl} decreases in the presence of this inhibitor. The decrease in C_{dl} , which can result from a decrease in local dielectric constant and/or an increase in the thickness of the electric double layer [13- 14], suggested that BPP molecules function by adsorption at the metal/solution interface. Thus, the decrease in C_{dl} values and the increase in R_t values and consequently of inhibition efficiency may be due to the gradual replacement of water molecules by the adsorption of the BPP molecules on the metal surface, decreasing the extent of dissolution reaction [15-16].

3.3 Weight loss, corrosion rates and inhibition efficiency

The effect of the addition of BPP tested at different concentrations on the corrosion of C38 steel in 0.5M H_2SO_4 solution was studied by using weight-loss at 298 K. Inhibition efficiency E_w (%) is calculated as follows:

$$EI_w (\%) = \frac{W_{corr} - W'_{corr}}{W_{corr}} \times 100 \quad (5)$$

where W_{corr} and W'_{corr} are the corrosion rates of C38 steel due to the dissolution in 0.5 M H_2SO_4 in the absence and the presence of definite concentration of inhibitor, respectively.

Table 3. Effect of BPP concentration on corrosion data of C38 steel in 0.5 M H_2SO_4

Inhibitor	Conc. (M)	W_{corr} (mg. cm^{-2})	E_w (%)
Blank	1.0	1.00	----
BPP	1×10^{-3}	7.63	86.88
	1×10^{-4}	4.80	79.16
	1×10^{-5}	3.75	73.31
	1×10^{-6}	3.42	70.72

From this table we can see that the inhibition efficiency increases with the increasing inhibitor concentration. At this purpose, one observes that the optimum concentration of inhibitor required to achieve the efficiency is found to be 10^{-3} M ($P=86.88$ %).

The results obtained by this method are in good agreement with the values of inhibitor efficiency obtained from electrochemical measurements.

3.4. Adsorption and thermodynamic considerations

Basic information on the interaction between the organic compounds and metal surfaces can be provided from the adsorption isotherms. The values of surface coverage, θ , corresponding to different

concentrations of inhibitors at 298K have been used to explain the best isotherm to determine the adsorption isotherm. The adsorption isotherms generally considered were :

Temkin isotherm : $\exp(f.\theta) = K_{ads} \cdot C_{inh}$

Langmuir isotherm : $\frac{\theta}{1-\theta} = K_{ads} \cdot C_{inh}$

Frumkin isotherm : $\frac{\theta}{1-\theta} \cdot \exp(-2f.\theta) = K_{ads} \cdot C_{inh}$

Freundluich isotherm: $\theta = K_{ads} \cdot C_{inh}$

where K_{ads} is the equilibrium constant of the inhibitor adsorption process, C_{inh} the inhibitor concentration and f is the factor of energetic inhomogeneity, the surface coverage (θ) can obtain from weight loss measurements, it calculated by the following equation:

$$\theta = \frac{W_{corr} - W'_{corr}}{W_{corr}} \tag{6}$$

For BPP, the plot of C_{inh}/θ versus C_{inh} yielded straight line with slope value of 1.11. This slope is close to 1, and the strong correlation ($R^2 > 0.99995$) proved clearly that the adsorption of the BPP from 0.5 M H_2SO_4 solution on the C38 steel obeys the Langmuir adsorption isotherm where,

$$\frac{C}{\theta} = \frac{1}{K_{ads}} + C \tag{7}$$

with
$$K_{ads} = \frac{1}{55,5} \exp\left(-\frac{\Delta G^0_{ads}}{RT}\right) \tag{8}$$

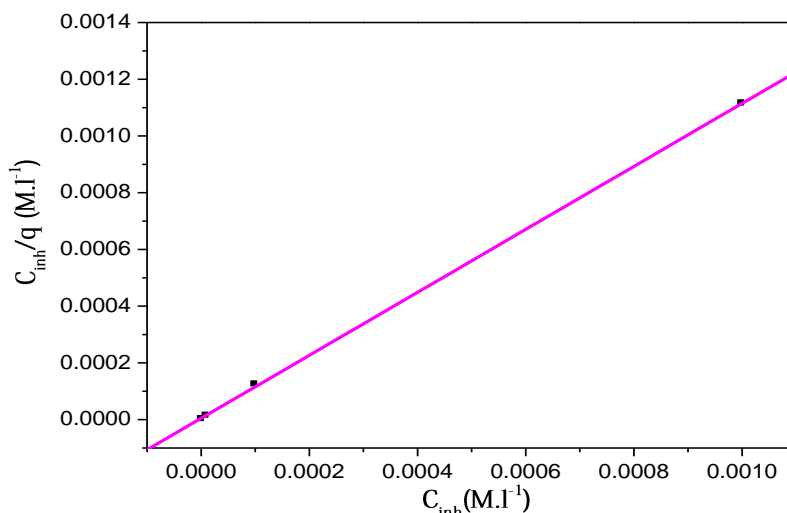


Figure 5. Langmuir adsorption of BPP on the C38 steel surface in 0.5 M H_2SO_4 solution.

The value of equilibrium adsorption constant obtained from this isotherm is about $2.1 \times 10^5 M^{-1}$, suggesting a chemically adsorbed film [17]. Moreover, the largest negative values of ΔG_{ads} , i.e. -40.31 kJ/mol for BPP, indicate that this inhibitor is strongly adsorbed onto the C38 steel surface. It is well known that values of $-\Delta G_{ads}$ of the order of 20 kJ/mol or lower indicate a physisorption; those of order

of 40 kJ/ mol or higher involve charge sharing or a transfer from the inhibitor molecules to the metal surface to form a co-ordinate type of bond [18-19].

We can note that a plausible mechanism of corrosion inhibition of C38 steel in 0.5 M H₂SO₄ by the compounds under study may be deduced on the basis of adsorption. In acidic solutions, these inhibitors can exist as cationic species which may be adsorbed on the cathodic sites of the C38 steel and reduce the evolution of hydrogen. The protonated inhibitor can also be adsorbed on the metal surface on specifically adsorbed sulfate ions, which act as a bridge between the metal surface and the electrolyte. Moreover, the adsorption of these compounds on anodic sites through lone pairs of electrons of nitrogen atoms and through phenyl group will then reduce the anodic dissolution of C38 steel [20-21].

3.5. Effect of temperature

In order to study the effect of temperature on corrosion inhibition of C38 steel in the acid reaction and to determine the activation energy of the corrosion process, the impedance measurements at various temperatures (298-328 K) in the absence and in the presence of BPP at optimal concentration (Figures 6 and 7).

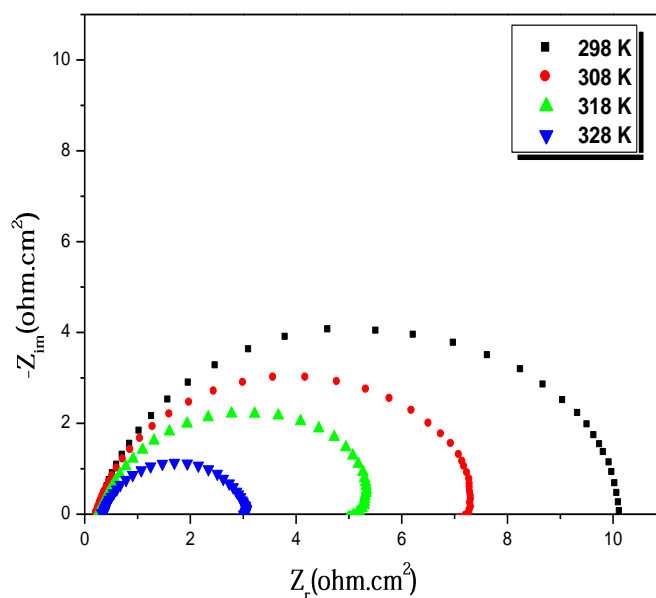


Figure 6. Nyquist diagrams for C38 steel in 0.5 M H₂SO₄ at different temperatures.

The corresponding results are given in table 4. We note that In the studied temperature range (298 -328 K) the charge transfer resistance decreases with increasing temperature both in uninhibited and inhibited solutions and the values of the inhibition efficiency of BPP are nearly constant and these results confirm that BPP acts as an efficient inhibitor in the range of temperature studied. The BPP inhibitor efficiency was temperature independent.

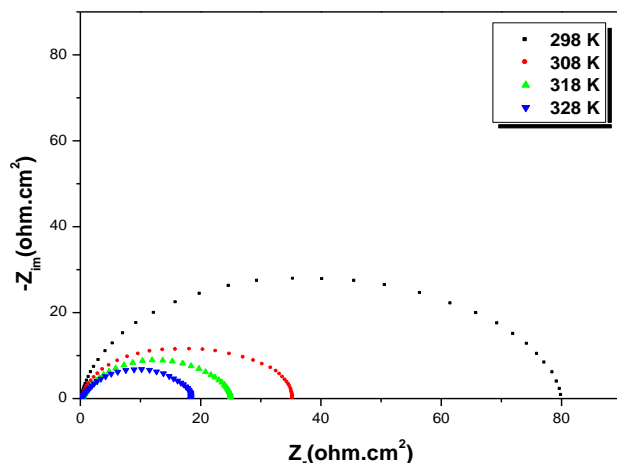


Figure 7. Nyquist diagrams for C38 steel in 0.5 M H₂SO₄ + 10⁻³ M of BPP at different temperatures.

Table 4. Thermodynamic parameters for the adsorption of BPP in 0.5 M H₂SO₄ on the C38 steel at different temperatures.

Inhibitor	Temperature (K)	R _t (Ω.cm ²)	f _{max} (Hz)	C _{dl} (μF/cm ²)	EI _{Rt} (%)
Blank	298	10	158	101	---
	308	7	200	114	---
	318	5	250	127	---
	328	3	632	84	---
10 ⁻³ M of BPP	298	80	63	31	87.50
	308	35	79	57	80.00
	318	25	100	64	80.00
	328	18	100	88	83.33

On the other hand, the values of R_t were employed to calculate values of the corrosion current density (I_{corr}) at various temperatures in absence and presence of BPP using the following equation [22]:

$$I_{corr} = RT(zFR_t)^{-1} \tag{9}$$

where R is the universal gas constant (R = 8.31 J K⁻¹mol⁻¹), T is the absolute temperature, z is the valence of iron (z = 2), F is the Faraday constant (F = 96.485 coulomb) and R_t is the charge transfer resistance.

The activation parameters for the corrosion process were calculated from Arrhenius type plot according to the following :

$$\log I = -\frac{E_a}{2.303 RT} + \log A \tag{10}$$

where E_a is the apparent activation corrosion energy, T is the absolute temperature, k is the Arrhenius pre-exponential constant and R is the universal gas constant.

And the an alternative formulation of Arrhenius equation is:

$$I_{corr} = \frac{RT}{Nh} \exp\left(\frac{\Delta S_a^0}{R}\right) \exp\left(-\frac{\Delta H_a^0}{RT}\right) \quad (11)$$

where h is Planck's constant, N is Avagadro's number, ΔS_a is the entropy of activation and ΔH_a is the enthalpy of activation.

The variations of logarithm of the corrosion rate of C38 steel ($\log I$) in sulfuric acid containing the optimal concentration of BPP and $\log(I/T)$ with reciprocal of the absolute temperature are presented in Figures 8 and 9, respectively. Straight lines with coefficients of correlation ($c. c$) higher to 0.99 are obtained.

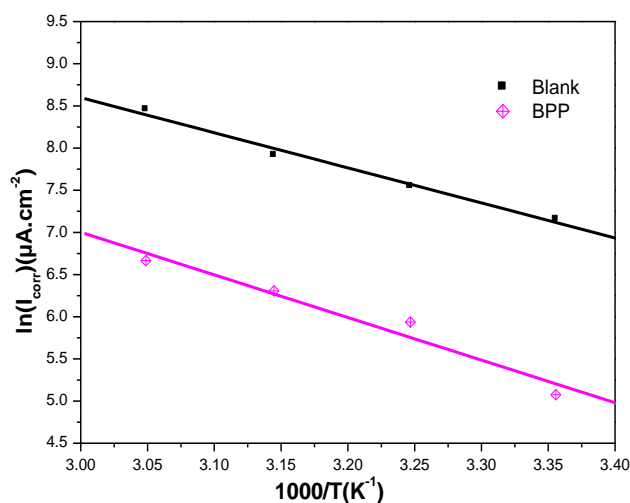


Figure 8. Arrhenius plots of C38 steel in 0.5 M H₂SO₄ with and without 10⁻³M of BPP

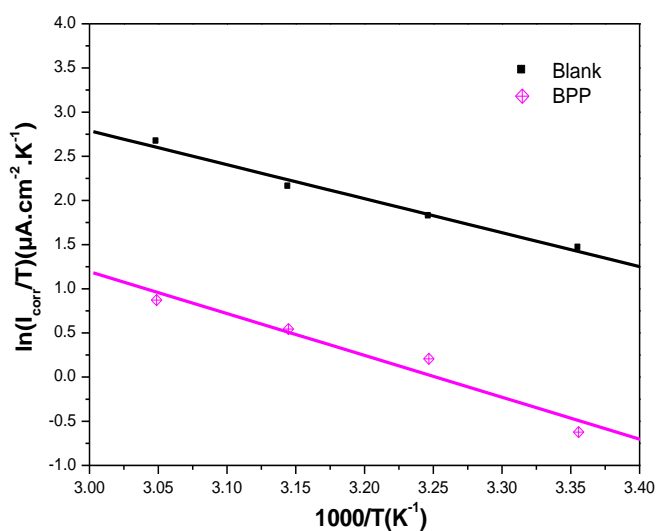


Figure 9. Arrhenius plots of C38 steel in 0.5 M H₂SO₄ with and without 10⁻³M of BPP

The E_a , ΔH_a and ΔS_a values were determined from the slopes of these plots. The calculated values of E_a , ΔH_a and ΔS_a in the absence and the presence of 10^{-3} M of BPP are given in table 5.

Table 5. The value of activation parameters for C38 steel in 0.5 M H_2SO_4 in the absence and presence of 10^{-3} M of BPP.

Inhibitor	E_a (kJ/mol)	ΔH_a (kJ/mol)	ΔS_a (J/mol)	$E_a - \Delta H_a$ (KJ/mol)
Blank	34.57	31.97	-78.35	2.6
BPP	42.00	39.39	-69.35	2.6

Inspection of these data reveals that the apparent activation energy E_a in 0.5 M H_2SO_4 solution in the absence of the BPP was 34.57 kJ/mol. The addition of BPP to the acid solution increases the activation energy.

On the other hand, the inspection of the same table revealed that the thermodynamic parameters (ΔS_a and ΔH_a) for dissolution reaction of C38 steel in 0.5 M H_2SO_4 in the presence of inhibitor are lower than that obtained in the absence of inhibitor. The positive sign of ΔH_a reflects the endothermic nature of the C38 steel dissolution process suggesting that the dissolution of C38 steel is slow [23] in the presence of inhibitor. Large and negative value of entropies (ΔS_a) imply that the activated complex in the rate determining step represents an association rather than a dissociation step [24], meaning that a decrease in disordering takes place on going from reactants to the activated complex [25-26].

4. CONCLUSIONS

BPP was demonstrated to be a good inhibitor for the corrosion of C38 steel at different temperatures in 0.5 M H_2SO_4 . The inhibition efficiency increases with increasing inhibitor concentration and increases slightly with increasing temperature. BPP acts as a mixed-type corrosion inhibitor, inhibiting the anodic and cathodic processes of the corrosion reactions by forming a protective film on the metal surface. The adsorption model was found to obey the Langmuir adsorption isotherm. The phenomenon of chemical adsorption is proposed from the value of ΔG_{ads} obtained, and the adsorption process is spontaneous.

ACKNOWLEDGEMENTS

The authors extend their sincere appreciation to the Deanship of Scientific Research at King Saud University for funding the work through the research group project No. RGP-VPP-089.

References

1. A. Anejjar, R. Salghi, A. Zarrouk, H. Zarrok, O. Benali; B. Hammouti, S. S. Al-Deyab, B. Benchat, R.; Saddik, *Res Chem Intermed.*, 2013, DOI 10.1007/s11164-013-1244-7.

2. M. Elayyachy, A. El Idrissi, B. Hammouti, *Corros. Sci.* 48 (2006) 2470-2479.
3. S. Merah, L. Larabi, O. Benali, Y. Harek, *Pig. Res. Tech.*, 37(5) (2008) 291–298.
4. O. Benali, L. Larabi, Y. Harek, *J. App. Electrochem.*, 39 (2009) 769-778.
5. D. Ben Hmamou, R. Salghi, A. Zarrouk, O. Benali, H. Zarrok, B. Hammouti, S. S. Al-Deyab, *Res. Chem. Intermed.*, 2012, DOI 10.1007/s11164-012-0892-3.
6. H. Zarrok; A. Zarrouk, R. Salghi, M. Assouag, B. Hammouti, H. Oudda, S. Boukhris, S. S. Al Deyab, I. Warad, *Der Pharmacia Lett.*, 5 (2) (2013) 43-53.
7. H. Oudda, A. Zarrouk, R. Salghi, B. Hammouti, M. Ebn Touhami, S. S. Al-Deyab, H. Zarrok, *GU. J. Sci.*, 26(1) (2013) 21-29.
8. O. Benali, M. Ouazene, *Arab J. Chem.*, 4 (2011) 443–448.
9. H. B. Ouici, O Benali, Y. Harek, L. Larabi, B. Hammouti, A. Guendouzi, *Res. Chem. Intermed.*, 39 (2013) 2777–2793.
10. D. Ben Hmamou, M. R. Aouad, R. Salghi, A. Zarrouk, M. Assouag, O. Benali, M. Messali, H. Zarrok, B. Hammouti, *J. Chem. Pharma. Res.*, 4 (7) (2012) 3489-3497.
11. Q. B. Zhang, Y. X. Hua, *Electrochim. Acta*, 54 (2009) 1881–1887.
12. L. Larabi, O. Benali, Y. Harek, *Mater. Lett.*, 61 (2007) 3287-3291.
13. O. Benali, L. Larabi, M. Traisnel, L. Gengembre, Y. Harek, *Appl. Surf. Sci.*, 253 (2007) 6130-6139.
14. E. McCafferty, N. Hackerman, *J. Electrochem. Soc.*, 119 (1972) 146-154.
15. F. Bentiss, M. Traisnel, M. Lagrenée, *Corros. Sci.*, 42 (2000) 127-146.
16. S. Muralidharan, K.L.N. Phani, S. Pitchumani, S. Ravichandran, S.V.K. Iyer, *J. Electrochem. Soc.*, 142 (1995) 1478-1483.
17. L. Larabi, Y. Harek, O. Benali, S. Ghalem, *Prog. Org. Coat.*, 54 (2005) 256–262.
18. A. Dadgarinezhad, F. Baghaei, *GU. J. Sci.*, 24(2) (2011) 219-226
19. V. R. Saliyan, A. V. Adhikari, *Bull. Mater. Sci.*, 31 (4) (2008) 699–711.
20. A. H. Al Hamzi, H. Zarrok, A. Zarrouk, R. Salghi, B. Hammouti, M. Bouachrine, A. Amine, F. Guenoun, H. Oudda, *Der Pharma. Lett.*, 5 (2) (2013) 27-39.
21. A. H. Al Hamzi, H. Zarrok, A. Zarrouk, R. Salghi, B. Hammouti, S.S. Al-Deyab, M. Bouachrine, A. Amine, F. Guenoun, *Int. J. Electrochem. Sci.*, 8 (2013) 2586 – 2605.
22. F. Beck, U. A. Kruger, *Electrochim. Acta*, 41 (1996) 1083.
23. N. M. Guan, L. Xueming, L. Fei, *Mater. Chem. Phys.*, 86 (2004) 59-68.
24. V. R. Saliyan, A. V. Adhikari, *Bull. Mater. Sci.*, 31 (4) (2008) 699–711.
25. J. Marsh, *Advanced Organic Chemistry* 3rd ed., Wiley Eastern New Delhi, 1988.
26. F. Bentiss, M. Traisnel, M. Lagrenée, *Corros. Sci.*, 47 (2005) 2915-2931.